Dentomaxillofacial Radiology (2004) 33, 83–86
© 2004 The British Institute of Radiology
http://dmfr.birjournals.org

RESEARCH

Radiation exposure during midfacial imaging using 4- and 16-slice computed tomography, cone beam computed tomography systems and conventional radiography

D Schulze*[,1], M Heiland[2], H Thurmann[3] and G Adam[4]

[1]*Department of Oral Radiology, University Hospital Hamburg-Eppendorf, Hamburg, Germany;* [2]*Department of Oral and Maxillofacial Surgery, University Hospital Hamburg-Eppendorf, Hamburg, Germany;* [3]*Department of Radiation Therapy, University Hospital Hamburg-Eppendorf, Hamburg, Germany;* [4]*Department of Diagnostic and Interventional Radiology, University Hospital Hamburg-Eppendorf, Hamburg, Germany*

Objectives: Radiation doses were determined to balance risks against usefulness of the different modalities available for the imaging of the facial skeleton.
Methods: An Alderson Rando Phantom, armed with lithium fluoride thermoluminescent dosemeters (TLDs) was exposed using a set of four conventional radiographs (orbital view, modified Waters view, orthopantomography, skull posterior–anterior 0°), two different cone beam computed tomography (CBCT) (NewTom 9000 and Siremobil Iso-C^{3D}), and multislice computed tomography (CT) modalities (Somatom VolumeZoom and Somatom Sensation 16). TLDs from 14 well defined anatomical sites lying within the primary beam as well as the TLD corresponding to the thyroid gland were evaluated.
Results: Multislice CT showed the highest exposure values. Exposure levels of the CBCT sytems lay between CT and conventional radiography. Dose measurement for the 16-slice CT revealed nearly the same radiation exposure as the 4-slice system when adapted examination protocols were used.
Conclusions: Selection of the most appropriate imaging modality should be performed in view of the delivered doses, required image quality and information and the clinical circumstances.
Dentomaxillofacial Radiology (2004) **33,** 83–86. doi: 10.1259/dmfr/28403350

Keywords: radiation exposure; computed tomography; cone beam computed tomography; conventional radiography

Introduction

Imaging of midfacial osseous structures can be performed using different techniques. Because they are based on different technical principles, image quality and applied radiation doses vary. Routinely a set of four conventional images are obtained serving as an overview including a panoramic radiograph, orbital view, modified Waters view and a submentovertex radiograph. Better information regarding osseous structures can be obtained with the NewTom 9000 (NIM s.r.l., Verona, Italy), which is based on the cone beam computed tomography (CBCT).[1] As previously reported, an isocentric mobile C-arm system, also based on CBCT and suitable for imaging of the facial skeleton (Siremobil Iso-C^{3D}; Siemens Medical Solutions, Erlangen, Germany), has been introduced especially for intraoperative imaging.[2,3] Intraoperative CT imaging of the head and neck region proves helpful during the reduction and fixation of orbitozygomatic fractures.[4–6] However, three-dimensional (3D) imaging of soft tissue with X-rays is only possible using CT, with multidetector systems representing the state of the art. Recently, 16-slice CT scanners have been introduced.[7]

Additionally, during dental implant planning, conventional radiography may be complemented by a CT scan. To what extent this is necessary, especially in respect to the unavoidable additional radiation exposure, is the basis for many critical discussions. On the other hand, it has to be kept in mind that during visualization of the midface region, sensitive structures like the lens of the eye are exposed to radiation, whereas for dental implantation this region can be omitted. In the case of CT, CTDI (CT Dose Index) and multiscan average dose (MSAD), the quantitative dose, have been defined, enabling manufacturer and projection independent evaluations.[8] However,

*Correspondence to: Dr Dirk Schulze, Department of Oral Radiology, University Hospital Hamburg-Eppendorf, Martinistr. 52, D- 20246 Hamburg, Germany; E-mail: dschulze@uke.uni-hamburg.de
Received 14 June 2003; revised 24 February 2004; accepted 24 February 2004

variations in dose by a factor of two or more using same the CT systems in standard head imaging have been described.[9] To evaluate radiation exposure of the different available modalities during imaging of the head and neck, clinical protocols for midfacial imaging were applied to an Alderson Rando Phantom.

Materials and methods

Radiation exposure was determined using a head and neck Alderson Rando phantom (Machlett, Springdale, CA) which contains ten axial sections with a thickness of 2.5 cm, each with 7 mm diameter holes for the insertion of thermoluminescent dosemeter (TLD) holder pins. The phantom consists of isocyanate rubber equivalent to human soft tissues in atomic number and density. For all the examinations, the axial sections 0 to 9 were used, armed with 194 lithium fluoride TLDs (LiF TLD-100, rods, diameter 1 mm, height 6 mm) obtained from Thermo Eberline Trading GmbH (Wermelskirchen, Germany). The rods were annealed (Annealing Oven PTW-O; Fa. Physikalisch-Technische Werkstätten, Freiburg, Germany) for 1 h at 400°C and stabilized at 100°C for another 3 h. Three rods were incorporated in each TLD holder pin. TLDs were placed in 13 well defined anatomical positions in the phantom, all lying within the primary beam. TLDs representing the thyroid glands and the lens were also placed on the phantom. Within 15–18 h after exposure the TLDs were tempered for 1 h at 100°C and then read out with a Harshaw 5500 TLD-Reader (Thermo Eberline Trading GmbH). The day after the readout of measurements the detector groups were incorporated into a solid body phantom and exposed to a linear accelerator (6 MV X-ray). The geometry equaled a water depth of 0.05 m. The values so acquired were used as calibrations for each detector individually and correlated with the measurement values. Dosimetry values were determined from these after correction with known correction factors for energy sensibility.

There is a linear relationship of the correction factor for energy dependence between 0.68 and 0.75 at tube voltages between 63 kV and 120 kV. For a linac calibration radiation (6 MV) the calibration factor is 1.00.

The dose values were determined as water energy doses related on ^{60}Co radiation. This may be traced back through measurements with ionisation chambers to the national institute on technical units (Physikalisch-Technische Bundesanstalt, Braunschweig, Germany).

Panoramic examinations were conducted using the Orthophos (Sirona, Bensheim, Germany). The other conventional images (modified Waters view, Orbita, skull posterior–anterior (PA) 0°) were performed with the Orbix (Siemens–Elema AB, Göteborg, Sweden). For equilibration of radiation exposure of the TLD, the set of conventional imaging was obtained with the same tube voltage (77 kV). Furthermore, because conventional axial imaging of the Alderson Rando phantom was not possible, instead of the submentovertex radiograph that is usually performed to visualize both zygomatic arches the skull, PA 0° projection was included in the set of conventional images.

The Siremobil Iso-C^{3D} is based on the isocentric fluoroscopy system Siremobil Iso-C. Via a 190° automatic orbital rotation 100 isocentric projections are generated.

The NewTom 9000 uses a 360° rotation while generating 360 single projections. The phantom was positioned in both systems of CBCT to enable the visualization of the orbit, maxillary sinus, upper and lower jaw including both mandibular condyles.

CT images (Somatom VolumeZoom; Siemens Medical Solutions), were generated according to the modified orbita/sinus protocol. Including the latest generation of CT scanners, the evaluation was repeated with a 16-slice scanner (Somatom Sensation 16; Siemens Medical Solutions). The borders of the field of view were defined just to include the frontal sinus and the mandible in both examinations.

A comparison of image quality is not included in this study.

Table 1 summarizes the details of the different imaging modalities.

Finally, the average dose values were determined for all chosen anatomical landmarks.

Results

The highest dose occurred during CT imaging. The highest value was measured in the right vitreous body. Both CT scanners led to comparable levels of radiation exposure (Figure 1).

Depending on the number of primary fluoroscopic shots used, lower dose levels were observed during the

Table 1 Measurement overview

	No. of exposures	*Exposure time (s)*	*kV*	*mA*	*Slice thickness (mm)*	*Collimation (mm)*	*Pitch (mm)*
Conventional imaging							
• orthopantomography	10	13.3	77	14			
• modified Waters view	10	0.2	77	30.5			
• orbital view	10	0.18	77	25.5–26.5			
• Skull PA 0°	10	0.2	77	17.5			
Siremobil Iso-C^{3D}	20	18	59–72	2.5–3.5 per shot			
NewTom 9000	5	76	110	122–155			
Volume Zoom	8		120	60	3.0	1.0	3.5
Sensation 16	10		120	60	4.0	0.75	5.0

PA, posterior–anterior

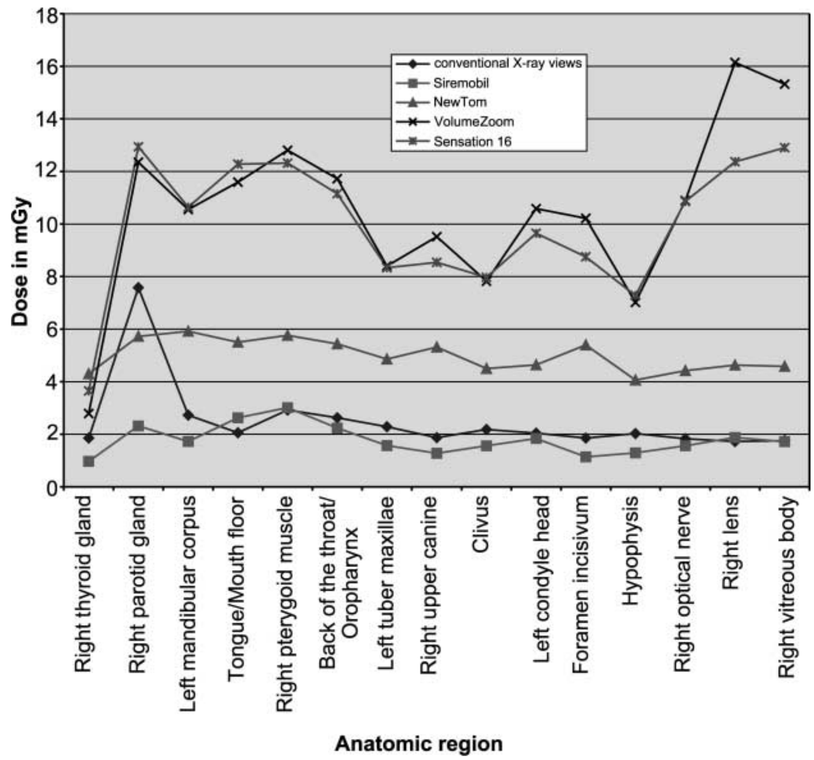

Figure 1 Radiation exposure in mGy

CBCT. For the NewTom 9000, these values were twice to three times higher than those observed while using the Siremobil Iso-C^{3D}.

During imaging using the NewTom 9000, the greatest radiation exposure was noted in the vicinity of the mandibular corpus, whereas the Siremobil Iso-C^{3D} produced the highest measured dose in the region of the pterygoid muscle (Table 2).

The necessary dose administered during the use of the Siremobil Iso-C^{3D} was comparable with the doses experienced during conventional imaging. Surprisingly, a high dose was measured in the area of the right parotid gland in the latter examination.

Discussion

Currently, there are several methods available to facilitate midfacial imaging. The indication for the use of each imaging modality varies. If pathologies associated with trauma need to be highlighted, the imaging of osseous structures is of primary importance. All the previously mentioned diagnostic methods are applicable, although the CT scan gives rise to the best 3D images. For featuring high contrasting structures, typical of osseous structures, the CBCT also proves well suited.

For tumour derived alterations, the CT scan proves most suitable, with its capacity of soft tissue reconstruction. Conventional radiography or the CBCT on the other hand, can only visualize primary osseous tumours or, indirectly, soft tissue tumours via osseous destruction of an impinging tumour. Decisive for the choice of method is not only the applicability during traumatological evaluation or pre-operative diagnosis but also the expected radiation exposure of each system.

In order to compare radiation exposure from different imaging modalities to limited exposed areas, radiation exposure of single TLDs using the same methods of determination are shown instead of calculated effective dosages. Generally, it has to be emphasized that radiation exposure values differ even in the literature depending not only on scanning parameters and positioning of the phantom but on the methods of analysis as well. Information on values of state of the art multislice CT scanners are limited compared with literature values obtained with single slice scanners. Furthermore, many reports dealt with radiation exposure in dental implant radiography exposing upper and lower jaw separately.[10–12] However, radiation exposure of the mandible with our midfacial CT protocol was between normal and low dental CT values obtained with single slice CT.[13]

At first look, the CBCT systems differ in respect to the dosimetric parameter. However, it should be kept in mind that different numbers of fluoroscopic shots are used.

Surprisingly, the doses of the conventional radiography and of the Siremobil Iso-C^{3D} are equivalent. The high value measured in the region of the parotid gland using the combination of conventional images seems to result from panoramic radiography, because Cohnen et al showed that orthopantomography alone also results in higher doses in

Table 2 Radiation exposure in mGy

Anatomic region	*Conventional X-ray views*	*Siremobil*	*NewTom*	*Volume Zoom*	*Sensation 16*
Right thyroid gland	1.86	0.97	4.3	2.79	3.65
Right parotid gland	7.58	2.32	5.72	12.35	12.94
Left mandibular corpus	2.73	1.725	5.92	10.55	10.64
Tongue/oral floor	2.06	2.63	5.5	11.59	12.28
Right pterygoid muscle	2.92	3.01	5.76	12.81	12.32
Back of the throat/oropharynx	2.63	2.235	5.44	11.72	11.15
Left tuber maxillae	2.29	1.575	4.86	8.4	8.34
Right upper canine	1.87	1.275	5.32	9.52	8.54
Clivus	2.18	1.56	4.5	7.82	7.97
Left mandibular condyle	2.04	1.84	4.64	10.58	9.65
Foramen incisivum	1.86	1.14	5.4	10.22	8.75
Hypophysis	2.03	1.295	4.06	7.02	7.28
Right optical nerve	1.83	1.56	4.42	10.89	10.86
Right lens	1.725	1.8775	4.63	16.14	12.37
Right vitreous body	1.76	1.715	4.58	15.32	12.90

the parotid/mandibular angle region.[14] However, the level of values in this study was below our results, probably because the mean of only two measurements has been shown.

In clinical settings not absolute values of radiation exposure, but the proportion of exposures of available modalities should be kept in mind. Selection of the most appropriate imaging modality should be performed in view of the delivered doses, required image quality and information and the clinical circumstances. Subsequently, it must be assumed that in the future, in a large number of the traumatological queries a CBCT will primarily be advocated. Furthermore, as intraoperative 3D imaging using mobile CT scanners is increasingly described in midfacial trauma surgery,[4–6] 3D fluoroscopy offers an easily handled alternative with radiation exposure close to conventional imaging.

References

1. Mozzo P, Procacci C, Tacconi A, Martini PT, Bergamo Andreis IA. A new volumetric CT machine for dental imaging based on the cone-beam technique: preliminary results. *Eur Radiol* 1998; **8:** 1558–1564.
2. Linsenmaier U, Rock C, Euler E, Wirth S, Brandl R, Kotsianos D, et al. Three-dimensional CT with a modified C-arm image intensifier: feasibility. *Radiology* 2002; **224:** 286–292.
3. Heiland M, Schulze D, Adam G, Schmelzle R. 3D-imaging of the facial skeleton with an isocentric mobile C-arm system (Siremobil Iso-C^{3D}). *Dentomaxillofac Radiol* 2003; **32:** 21–25.
4. Stanley R. Use of intraoperative computed tomography during repair of orbitozygomatic fractures. *Arch Facial Plast Surg* 1999; **1:** 19–24.
5. Hoelzle F, Klein M, Schwerdtner O, Lueth T, Albrecht J, Hosten N, et al. Intraoperative computed tomography with the mobile CT Tomoscan M during surgical treatment of orbital fractures. *Int J Oral Maxillofac Surg* 2001; **30:** 26–31.
6. Hoffmann J, Krimmel M, Dammann F, Reinert S. Möglichkeiten der intraoperativen Diagnostik mit einem fahrbaren Computertomographen. *Mund Kiefer GesichtsChir* 2002; **6:** 346–350.
7. Flohr T, Stierstorfer K, Bruder H, Simon J, Schaller S. New technical developments in multislice CT. *Fortschr Röntgenstr* 2002; **174:** 839–845.
8. Shope T, Gagne R, Johnson G. A method for describing the doses delivered by transmission x-ray computed tomography. *Med Phys* 1981; **8:** 488–495.
9. McCrohan JL, Patterson JF, Gagne RM, Goldstein HA. Average radiation doses in a standard head examination for 250 CT systems. *Radiology* 1987; **163:** 263–268.
10. Kassebaum D, Stoller N, McDavid W, Goshorn B, Ahrens C. Absorbed dose determination for tomographic implant site assessment techniques. *Oral Surg Oral Med Oral Pathol* 1992; **73:** 502–509.
11. Ekestubbe A, Thilander A, Gröndahl K, Gröndahl HG. Absorbed doses from computed tomography for dental implant surgery: comparison with conventional tomography. *Dentomaxillofac Radiol* 1993; **22:** 13–17.
12. Bianchi J, Goggins W, Rudolph M. In vivo, thyroid and lens surface exposure with spiral and conventional computed tomography in dental implant radiography. *Oral Surg Oral Med Oral Pathol Oral Radiol Endod* 2000; **90:** 249–253.
13. Rustemeyer P, Streubühr U, Hohn HP, Rustemeyer R, Eich HT, John-Mikolajewski V, et al. Niedrigdosis Dental-CT. *Fortschr Röntgenstr* 1999; **171:** 130–135.
14. Cohnen M, Kemper J, Möbes O, Pawelzik J, Mödder U. Radiation dose in dental radiology. *Eur Radiol* 2002; **12:** 634–637.